

Analysis of V2V Broadcast Performance Limit for WAVE Communication Systems Using Two-Ray Path Loss Model

Yoo-Seung Song and Hyun-Kyun Choi

The advent of wireless access in vehicular environments (WAVE) technology has improved the intelligence of transportation systems and enabled generic traffic problems to be solved automatically. Based on the IEEE 802.11p standard for vehicle-to-anything (V2X) communications, WAVE provides wireless links with latencies less than 100 ms to vehicles operating at speeds up to 200 km/h. To date, most research has been based on field test results. In contrast, this paper presents a numerical analysis of the V2X broadcast throughput limit using a path loss model. First, the maximum throughput and minimum delay limit were obtained from the MAC frame format of IEEE 802.11p. Second, the packet error probability was derived for additive white Gaussian noise and fading channel conditions. Finally, the maximum throughput limit of the system was derived from the packet error rate using a two-ray path loss model for a typical highway topology. The throughput was analyzed for each data rate, which allowed the performance at the different data rates to be compared. The analysis method can be easily applied to different topologies by substituting an appropriate target path loss model.

Keywords: WAVE, IEEE 802.11p, ITS, V2V, Vehicular Communications, Telematics, Smart transportation.

Manuscript received June 17, 2016; revised Feb. 2, 2017; accepted Feb. 3, 2017. This work was supported by the ICT R&D program of MSIP/IITP (201500275, High Speed V-Link Communication Technology Development for Real Time Control of Autonomous Driving Vehicle).

Yoo-Seung Song (corresponding author, yssong00@etri.re.kr) and Hyun-Kyun Choi (choihk@etri.re.kr) are with the SW & Contents Research Laboratory, ETRI, Daejeon, Rep. of Korea

This is an Open Access article distributed under the term of Korea Open Government License (KOGL) Type 4: Source Indication + Commercial Use Prohibition + Change Prohibition (<http://www.kogl.or.kr/news/dataView.do?dataIdx=97>).

I. Introduction

The advent of wireless access in vehicular environments (WAVE) technology for high-speed vehicles has improved the intelligence and convenience of transportation systems. Vehicle-to-anything (V2X) communications using WAVE technology has become a solution that both alleviates or overcomes various traffic problems, and provides useful information for vehicle drivers, as shown in the context of an intelligent transportation system (ITS) in Fig. 1 [1].

WAVE is a dedicated short-range communications (DSRC) technology based on IEEE 802.11p, which is an approved amendment to the IEEE 802.11 standard that adds wireless access in vehicular environments [2]. The IEEE1609.x series of standards supports security, networking, and multichannel operations for higher layers. The IEEE 802.11p standard was designed for vehicular communications at speeds up to 200 km/h requiring latencies less than 100 ms [3].

Suppliers are now producing WAVE products, such as on-board units (OBUs) and roadside units (RSUs), for applications globally, and a variety of tests have been conducted for different configurations of several public road topologies [4]. In support of the prompt commercialization of WAVE technology, performance verification and trial services are underway in various countries. Research and development has been actively conducted in several projects, of which the safety pilot led by the Department of Transportation in the USA and Drive-C2X in Europe are the most well-known [5], [6].

The key performance parameters in WAVE are the throughput and delay because most of its applications require high capacity and low latency. The performance of WAVE has been investigated under various conditions and with different approaches. For example, performance evaluations of WAVE have been conducted based on field measurements. The results of testing in different highway scenarios are shown in [7] and

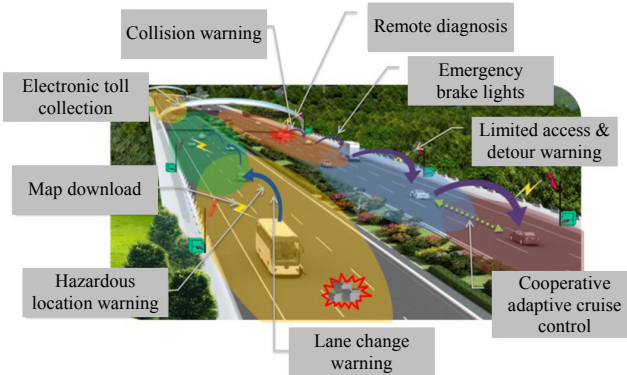


Fig. 1. Applications for ITS services using V2X WAVE technology.

[8], in which the V2X performance of the link coverage, link access time, throughput, and delay was evaluated as the vehicle speed and network load varied. In addition, the throughput and packet error rate (PER) were simulated in urban traffic and crowded and/or non-crowded highway scenarios in [9] and [10], respectively. The results were obtained in terms of the signal-to-noise ratio (SNR) and distance between vehicles.

A numerical analysis of the throughput and delay limit of IEEE 802.11a/b was studied in [11], where the maximum throughput and minimum delay were derived for different payload sizes and transmission rates. The effective packet transmission time and packet collision probability were derived to compute the throughput for the IEEE 802.11 system in [12]; however, the system configuration and channel mode were different from those used in WAVE systems. The authors in [13]–[15] show that the broadcast reception rate and delay in vehicular ad-hoc networks are severely degraded as the number of stations increases due to the small sized contention windows caused by packet collisions. Recent experimental results on the packet delivery rate for vehicle-to-vehicle (V2V) communications on typical urban highways were published in [16] and [17] for line-of-sight (LOS) and non-line-of-sight conditions. However, to the best of our knowledge, no studies have been published that present a numerical analysis of the broadcast throughput or link budget limit for the WAVE system using a path loss model.

In this paper, the maximum V2V broadcast throughput and link budget limit for WAVE systems are analyzed using a path loss model. First, the maximum throughput and minimum delay of the IEEE 802.11p frame format, and the upper bound of the PER for additive white Gaussian noise (AWGN) and fading channels, are described in Section II. Next, the V2V link budget limit, including the minimum sensitivity and maximum allowable path loss using a two-ray path loss model derived for AWGN and fading channels, is detailed in Section III. The maximum V2V broadcast throughput considering the PER and path loss performance described in the previous section is

provided in Section IV. Finally, some concluding remarks are given in Section V.

II. Performance Limit

1. Throughput and Delay Limit

It is difficult to analyze the maximum throughput performance for a real WAVE system where several vehicles are contending for a wireless medium. To derive the maximum throughput and minimum delay, the following assumptions are made to simplify the analysis: a channel is ideal without packet losses; there is only one vehicle that transmits packets and its queue is always full; all other vehicles can only receive packets in order to avoid packet collisions in the air; and finally, when an ACK frame transmission is required, the lowest data rate of 3 Mbps is used.

The physical layer convergence procedure protocol data unit (PPDU) format of the IEEE 802.11 PHY consists of a physical layer convergence procedure (PLCP) preamble, PLCP header, physical layer service data unit (PSDU) tail bits and pad bits, as shown in Fig. 2. The PSDU format includes a MAC header, frame body, and frame check sequence (FCS) field. The values of the time duration of T_{pm} , T_{sg} , and T_{da} , as well as other key

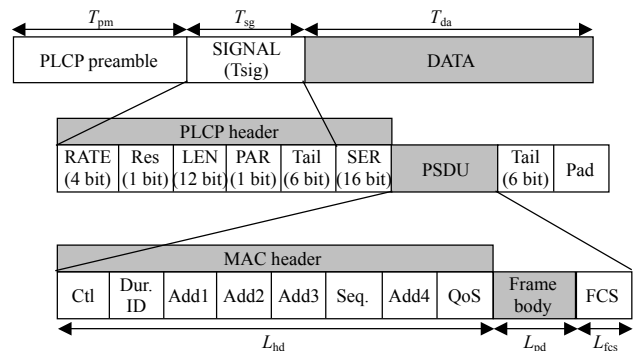


Fig. 2. PPDU frame format for IEEE 802.11p OFDM PHY.

Table 1. Parameters for IEEE 802.11a vs. IEEE 802.11p.

Parameter	802.11a	802.11p	Description
T_{slot}	9 μ s	13 μ s	Slot time
T_{SIFS}	16 μ s	32 μ s	SIFS time
T_{pm}	16 μ s	32 μ s	PLCP preamble duration
T_{sg}	4 μ s	8 μ s	Signal field duration
T_{DIFS}	34 μ s	58 μ s	DIFS time
T_{sym}	4 μ s	8 μ s	Symbol time
T_{grd}	0.8 μ s	1.6 μ s	Guard time
T_{prop}		1 μ s	Propagation time
CW_{min}		15	Contention window minimum size

Table 2. PSDU subfield size for the data and ACK frame.

Parameter	Size (bits)	Description
L_{hd}	32×8	Data MAC header
L_{pd}	$[0-2304] \times 8$	Data payload
L_{fcs}	4×8	FCS
L_{ack}	10×8	ACK MAC header

Table 3. PHY modes and N_{DBPS} of IEEE 802.11p.

Mode	Data rate (Mbps)	Modulation	Code rate	N_{DBPS}
1	3	BPSK	1/2	24
2	4.5	BPSK	3/4	36
3	6	QPSK	1/2	48
4	9	QPSK	3/4	72
5	12	16 QAM	1/2	96
6	18	16 QAM	3/4	144
7	24	64 QAM	2/3	192
8	27	64 QAM	3/4	216

parameters are summarized in Tables 1 and 2.

Based on the PPDU frame format, the data transmission duration for a given data rate mode can be expressed as

$$T_{\text{data}}^{\text{mode}} = T_{\text{pm}} + T_{\text{sg}} + T_{\text{sym}} \cdot \left[\frac{16 + L_{\text{hd}} + L_{\text{pd}} + L_{\text{fcs}} + 6}{N_{\text{DBPS}}^{\text{mode}}} \right], \quad (1)$$

where L_{hd} , L_{pd} , and L_{fcs} are the length of the MAC header for the data, payload, and FCS in bits, respectively. The term N_{DBPS} represents the number of data bits per OFDM symbol, the values of which are given in Table 3. Similarly, the ACK transmission duration for a given data rate mode can be written as

$$T_{\text{ack}}^{\text{mode}} = T_{\text{pm}} + T_{\text{sg}} + T_{\text{sym}} \times \left[\frac{16 + L_{\text{ack}} + L_{\text{fcs}} + 6}{N_{\text{DBPS}}^{\text{mode}}} \right], \quad (2)$$

where L_{ack} is the length of the MAC header for the ACK in bits.

The transmission cycle of the distributed coordination function in the IEEE 802.11 MAC consists of the distributed coordination function inter-frame space (DIFS) deferral, backoff/contention if necessary, data transmission, short inter-frame space (SIFS) deferral, and ACK transmission phase. Therefore, the maximum throughput can be written as

$$M_{\text{T,no_ack}}^{\text{mode}} = \frac{L_{\text{pd}}}{T_{\text{data}}^{\text{mode}} + T_{\text{ack}}^{\text{mode}} + 2T_{\text{prop}} + T_{\text{DIFS}} + T_{\text{SIFS}} + CW_{\text{avg}}}, \quad (3)$$

where the average backoff time $CW_{\text{avg}} = CW_{\text{min}} T_{\text{slot}} / 2$.

Because the broadcast does not require an ACK frame, the maximum throughput in (3) can be further simplified to

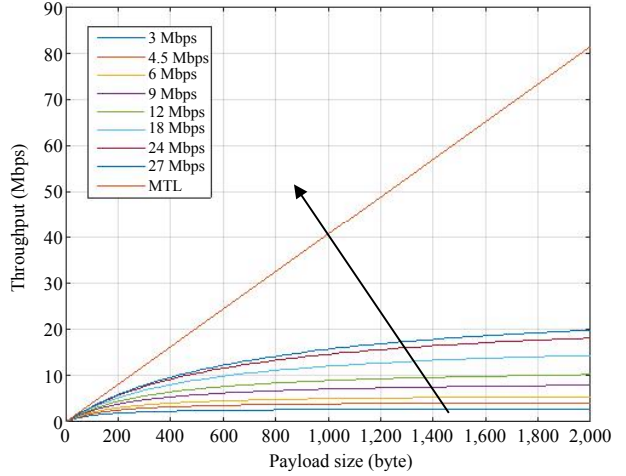


Fig. 3. Maximum throughput of the DSRC system for different PHY modes.

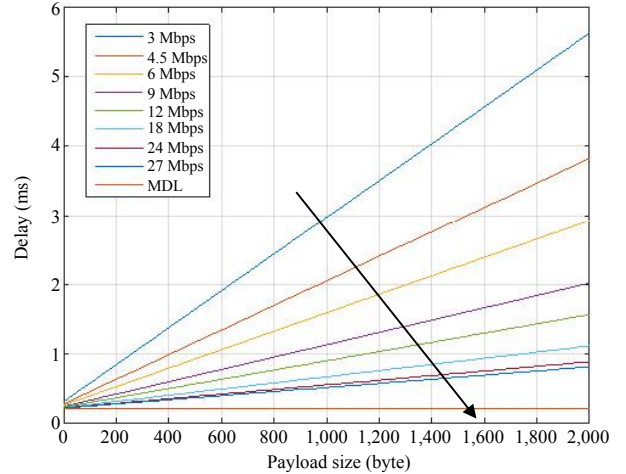


Fig. 4. Minimum delay of the DSRC system for different PHY modes.

$$M_{\text{T,no_ack}}^{\text{mode}} = \frac{L_{\text{pd}}}{T_{\text{data}}^{\text{mode}} + T_{\text{prop}} + T_{\text{DIFS}} + CW_{\text{avg}}}. \quad (4)$$

The packet delay is defined as the time duration of a packet transmission and its successful reception. The minimum delay is given by

$$M_{\text{D}}^{\text{mode}} = T_{\text{data}}^{\text{mode}} + T_{\text{prop}} + T_{\text{DIFS}} + CW_{\text{avg}}. \quad (5)$$

The results for the maximum throughput and minimum delay of IEEE 802.11p, as well as the maximum throughput limit (MTL) and minimum delay limit (MDL) are shown in Figs. 3 and 4, respectively. The MTL and MDL are obtained by assuming that the N_{DBPS} are infinite such that the time duration for a data transmission is zero. The maximum throughput of IEEE 802.11p is approximately 18 Mbps for the 27-Mbps PHY mode with a payload of 2,000 bytes, whereas the upper

limit is around 80 Mbps for an infinite data rate. The minimum delay is about 0.8 ms for 27-Mbps PHY mode with a payload of 2,000 bytes, whereas the lower limit is about 0.2 ms with an infinite data rate.

2. Upper Bound for Packet Error Probability

The error probability analysis for IEEE 802.11p was conducted for AWGN and Rayleigh fading channels.

A. Upper Bound of the PER in an AWGN Channel

The SNR of a received signal can be written as

$$\gamma = \frac{E_b}{N_0 B T_b}, \quad (6)$$

where E_b is the energy per bit, N_0 is the noise density in W/Hz, T_b is the transmission duration per bit, and B is the channel bandwidth in the IEEE 802.11p OFDM PHY. The SNR per bit is

$$\gamma_b = \frac{E_b}{N_0} = \gamma \cdot B T_b = \gamma \cdot \frac{B}{R}, \quad (7)$$

where $R = 1/T_b$ is the transmission bit rate in Mbps. The SNR per symbol is then given by

$$\gamma_s = \gamma_b \cdot k, \quad (8)$$

where k is the number of bits per modulated symbol. Because of the cyclic prefix (or guard time) for each OFDM symbol, the power loss a_g for each symbol should be considered. The power loss can be calculated from Table 1 as

$$a_g = \frac{T_{\text{sym}}}{T_{\text{sym}} + T_{\text{grd}}} \approx 0.8. \quad (9)$$

By considering the power loss in (9), the SNR per symbol becomes the average symbol energy per noise density, and is written as

$$\bar{\gamma}_s = a_g \cdot \gamma_s. \quad (10)$$

For an AWGN channel, the symbol error rate (SER) P_{sym} of all modulation schemes used in the 802.11p OFDM PHY can be derived from the SER of the N -ary pulse-amplitude modulation (N -PAM) as

$$P_{\text{sym}}^{N\text{-PAM}} = 2 \left(1 - \frac{1}{N} \right) Q \left(\sqrt{\frac{6}{N^2 - 1}} \cdot \bar{\gamma}_s \right), \quad (11)$$

where the Q -function is the tail probability of the standard normal distribution [18]. Because binary phase shift keying (BPSK) can be viewed as 2-ary PAM and has one bit per symbol, the bit error rate (BER) of BPSK is given by

$$P_{\text{bit}}^{\text{BPSK}} = P_{\text{sym}}^{\text{BPSK}} = P_{\text{sym}}^{\text{2-PAM}} = Q \left(\sqrt{2 \bar{\gamma}_s} \right). \quad (12)$$

The SER of the N -ary quadrature-amplitude modulation (N -QAM) scheme used in the 802.11p OFDM PHY can be written in PAM form as

$$P_{\text{sym}}^{N\text{-QAM}} = 1 - \left\{ 1 - 2 \cdot \left(1 - \frac{1}{\sqrt{N}} \right) \cdot Q \left(\sqrt{\frac{3}{N-1}} \bar{\gamma}_s \right) \right\}^2. \quad (13)$$

Based on the Gray code used in the 802.11p OFDM PHY, the BER of N -ary QAM can be written as [19]

$$P_{\text{bit}}^{N\text{-QAM}} \approx \frac{1}{\log_2 N} P_{\text{sym}}^{N\text{-QAM}}. \quad (14)$$

By substituting $N = 4, 16$, and 64 in (14) and assuming a high SNR for simplicity, the BER of quadrature phase shift keying (QPSK), 16 QAM, and 64 QAM is given respectively by

$$P_{\text{bit}}^{\text{QPSK}} \approx Q \left(\sqrt{\bar{\gamma}_s} \right), \quad (15)$$

$$P_{\text{bit}}^{\text{16QAM}} \approx \frac{3}{4} Q \left(\sqrt{\frac{1}{5} \bar{\gamma}_s} \right), \text{ and} \quad (16)$$

$$P_{\text{bit}}^{\text{64QAM}} \approx \frac{7}{12} Q \left(\sqrt{\frac{1}{21} \bar{\gamma}_s} \right). \quad (17)$$

The upper bound of the packet error probability for a packet length of L [bit] is given in [20] as

$$P_{\text{packet}}^{\text{mode}} (L) \leq 1 - \left(1 - \sum_{d=d_{\text{free}}}^{\infty} a_d \cdot P_d^{\text{mode}} \right)^L, \quad (18)$$

where P_d^{mode} is the probability of error in the pairwise comparison of two paths that differ in length by d bits. When Viterbi hard-decision decoding (HDD) is applied, it can be given as

$$P_d^{\text{mode}} = \begin{cases} \sum_{k=\frac{d+1}{2}}^d \binom{d}{k} (P_{\text{bit}}^{\text{mode}})^k (1 - P_{\text{bit}}^{\text{mode}})^{d-k}, & d = \text{odd}, \\ \sum_{k=\frac{d}{2}+1}^d \binom{d}{k} (P_{\text{bit}}^{\text{mode}})^k (1 - P_{\text{bit}}^{\text{mode}})^{d-k} \\ + \frac{1}{2} \binom{d}{d/2} (P_{\text{bit}}^{\text{mode}})^{\frac{d}{2}} (1 - P_{\text{bit}}^{\text{mode}})^{\frac{d}{2}}, & d = \text{even}. \end{cases} \quad (19)$$

The upper bound of the packet error rate can be approximated by considering the first few terms, which mostly dominate. The values of a_d and d_{free} for the convolutional encoder used in IEEE 802.11 OFDM PHY are shown in Table 4 [21], [22].

The upper bound of the PER is shown in Fig. 5 for an AWGN channel. The simulated packet length is 1,024 bytes, and Viterbi HDD is employed.

Table 4. Values of d_{free} and a_d for the convolutional encoder ($K = 7$) used in the IEEE 802.11 OFDM PHY, where the polynomials of g_0 and g_1 are 133 and 171, respectively.

Data rate (Mbps)	Coding rate (R)	d_{free}	$a_d, d = d_{\text{free}}, d_{\text{free}+1}, \dots$
3, 6, 12	1/2	10	{11, 0, 38, 0, 193, 0, 1331, 0, 7275, 0, ...}
4.5, 9, 18, 27	3/4	5	{8, 31, 160, 892, 4512, 23307, 121077, 625059, 3234886, 16753077, ...}
24	2/3	6	{1, 16, 48, 158, 642, 2435, 9174, 34705, 131585, 499608, ...}

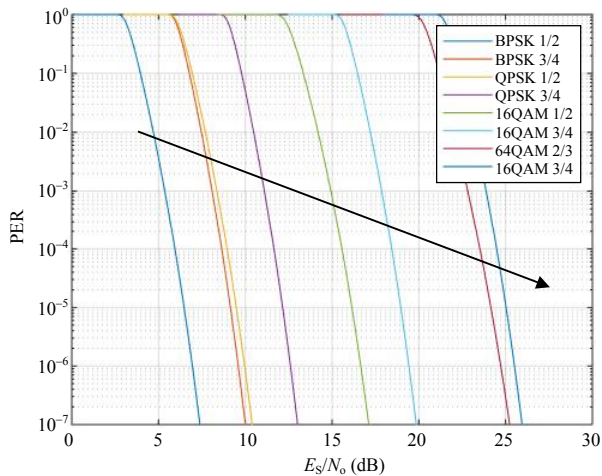


Fig. 5. PER in terms of E_s/N_o for the IEEE 802.11p OFDM PHY in an AWGN channel using a Viterbi HDD for the different modulation and coding schemes, where the packet length is 1,024 bytes.

B. Upper Bound PER under Rayleigh Fading Channel

The BER of IEEE 802.11p in a Nakagami- m fast fading channel was analyzed in [23]. A Rayleigh channel can be obtained from a Nakagami channel with $m = 1$. The average BER of BPSK with Viterbi HDD is given by

$$P_{\text{bit}}^{\text{BPSK}} = \frac{1}{2} \left(1 - \sqrt{\frac{\bar{\gamma}_s}{1 + \bar{\gamma}_s}} \right). \quad (20)$$

The average BER of N -ary QAM using a Viterbi HDD for IEEE 802.11p is given by

$$P_{\text{bit}}^{N\text{-QAM}} = 2 \left(\frac{\sqrt{N}-1}{\sqrt{N}} \right) \left(\frac{1}{\log_2 N} \right) \sum_{i=1}^{\sqrt{N}/2} \left(1 - \mu_i^{N\text{-QAM}} \right), \quad (21)$$

$$\text{where } \mu_i^{N\text{-QAM}} = \sqrt{\frac{1.5(2i-1)^2 \bar{\gamma}_s}{N-1+1.5(2i-1)^2 \bar{\gamma}_s}}. \quad (22)$$

The PER using a Viterbi HDD in a Rayleigh fading channel can be calculated using (18) through (21), the results of which are plotted in Fig. 6 for different data rate modes.

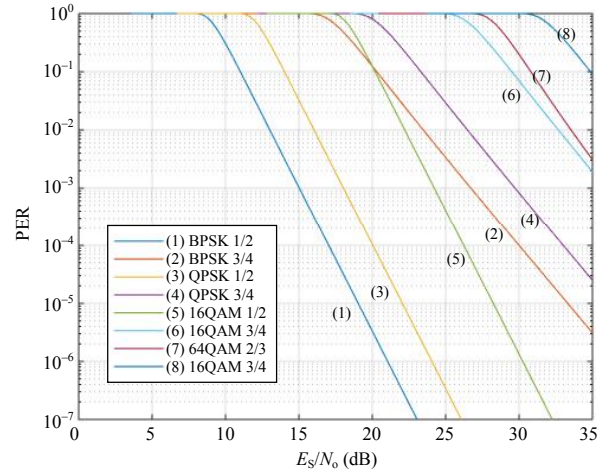


Fig. 6. PER of IEEE 802.11p for a Rayleigh fading channel using a Viterbi HDD for different modulation and coding schemes, where the packet length is 1,024 bytes.

III. V2V Link Budget

1. Path Loss Model

The two-ray path loss equation is used to model the power attenuation under highway conditions. This model considers a direct path (E_{LOS}) and a ground reflection path (E_{REF}). The received power [24] is given by

$$P_{\text{RX}} = |E_{\text{LOS}} + E_{\text{REF}}|^2, \quad (23)$$

and

$$= \left| \frac{\sqrt{P_{\text{TX}}}}{2\beta} \frac{1}{d_{\text{L}}} e^{-j\beta d_{\text{L}}} + \frac{\sqrt{P_{\text{TX}}}}{2\beta} \frac{1}{d_{\text{R}}} \frac{\varepsilon_{\text{r}} \cos \theta - \sqrt{\varepsilon_{\text{r}} - \sin^2 \theta}}{\varepsilon_{\text{r}} \cos \theta + \sqrt{\varepsilon_{\text{r}} - \sin^2 \theta}} e^{-j\beta d_{\text{R}}} \right|^2, \quad (24)$$

where P_{TX} is the transmitted power, $\beta = 2\pi/\lambda$, d_{L} is the LOS distance, d_{R} is the reflected ground distance, θ is the angle of incidence on a surface, and ε_{r} is the permittivity of the material. If we define the path loss PL as the received power over the transmitted signal power, (24) can be written as

$$PL = \left| \frac{1}{2\beta} \frac{1}{d_{\text{L}}} e^{-j\beta d_{\text{L}}} + \frac{1}{2\beta} \frac{1}{d_{\text{R}}} \frac{\varepsilon_{\text{r}} \cos \theta - \sqrt{\varepsilon_{\text{r}} - \sin^2 \theta}}{\varepsilon_{\text{r}} \cos \theta + \sqrt{\varepsilon_{\text{r}} - \sin^2 \theta}} e^{-j\beta d_{\text{R}}} \right|^2. \quad (25)$$

2. Receiver Sensitivity

The parameters in Table 5 are from the WAVE highway test site deployed in South Korea. The antenna gain of the OBU is omnidirectional, while that of the RSU is unidirectional. The power levels of the RSU and OBU are set to the maximum value. The equivalent isotropically radiated power (EIRP) is

Table 5. IEEE 802.11p/DSRC system link budget parameters.

Parameter	Value	Unit	Description
H_{RSU}	15	m	RSU height
P_{RSU}	17	dBm	RSU power
G_{RSU}	13	dBi	RSU antenna gain
$EIRP_{\text{RSU}}$	30	dBm	EIRP of RSU
G_{OBU}	7	dBi	OBU antenna gain
H_{OBU}	1.5	m	OBU height
P_{OBU}	16	dBm	OBU power
$EIRP_{\text{OBU}}$	23	dBm	EIRP of OBU
f_c	5.8	GHz	Center frequency
BW	10	MHz	Bandwidth

computed by adding the antenna gain to the maximum transmit power of each device.

The link budget is usually used to find the effective coverage of the communication link. The typical PL equation is given by

$$PL = S_{\text{RX}} - G_{\text{RX}} - E_{\text{TX}} \quad (26)$$

in dB, where S_{RX} , G_{RX} , and E_{TX} represent the receiver sensitivity, receiver antenna gain, and transmitter EIRP, respectively. Therefore, G_{RX} and E_{TX} will be replaced by G_{OBU} and $EIRP_{\text{OBU}}$ for the V2V scenario. The receiver sensitivity in terms of the SNR per symbol satisfying a specific PER is given by [25]

$$S_{\text{RX}} = -174 + NF + \left. \frac{\gamma_s}{k} \right|_{\text{PER}} + 10 \log_{10} R + ImpLoss \quad (27)$$

in dB, where NF , R , and $ImpLoss$ represent the noise figure and/or factor, the data rate, and the implementation loss, respectively. The PER with respect to the receiver sensitivity in Fig. 7 can be obtained from (18) and (27), where AWGN channel conditions are assumed, and the values of NF and $ImpLoss$ are set to 10 dB and 5 dB, respectively. Because QPSK 1/2 requires less bit energy than that of BPSK 3/4 to meet the same PER, the receiver sensitivity of QPSK 1/2 is better than that of BPSK 3/4. From Fig. 7, it can be seen that 64 QAM 3/4 PHY (MCS) mode requires a receiver sensitivity of -70 dBm to meet a PER of 10%, which is 20 dB higher than that of BPSK 1/2 mode.

The PER with respect to the receiver sensitivity is shown in Fig. 8 for a Rayleigh fading channel. Overall, the value of the receiver sensitivity under a fading channel is more than 15 dB worse compared to that of an AWGN channel. In addition, it was observed that the PHY mode with a coding rate of 1/2 outperforms that with a coding rate of 3/4.

Now, we can find the PER in terms of the PL by substituting (27) into (26), the results of which are plotted in Fig. 9 under

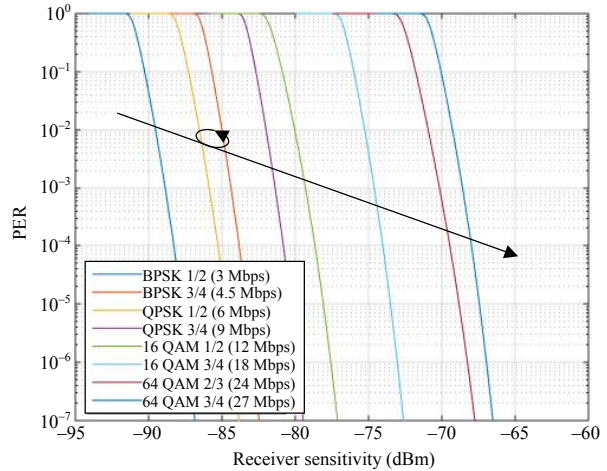


Fig. 7. PER vs. receiver sensitivity under AWGN channel, where NF and $ImpLoss$ are 10 dB and 5 dB, respectively.

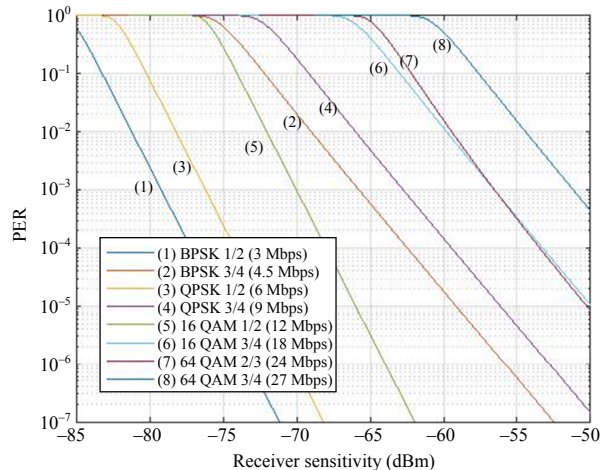


Fig. 8. PER vs. receiver sensitivity for a Rayleigh fading channel, where the NF and $ImpLoss$ are 10 dB and 5 dB, respectively.

the same conditions of:

$$PL = S_{\text{RX}} \left(\left. \frac{\gamma_s}{k} \right|_{\text{PER}} \right) - G_{\text{RX}} - E_{\text{TX}} \quad (28)$$

in dB. The link budget for BPSK 1/2 to meet a PER of 10% is around -120 dBm, whereas that of 64 QAM 3/4 is -100 dBm. The link budget of the PL is simply a shifted version of the received sensitivity based on the amount of the receiver antenna gain and EIRP of the transmitter, which increases the link budget and coverage.

A PER analysis in terms of the PL was performed for a Rayleigh fading channel, as shown in Fig. 10. The system obtained a higher margin through the gain in the receiver antenna and the transmit power.

We can also find the PER for a given V2V distance by making (25) and (28) have the same PL value.

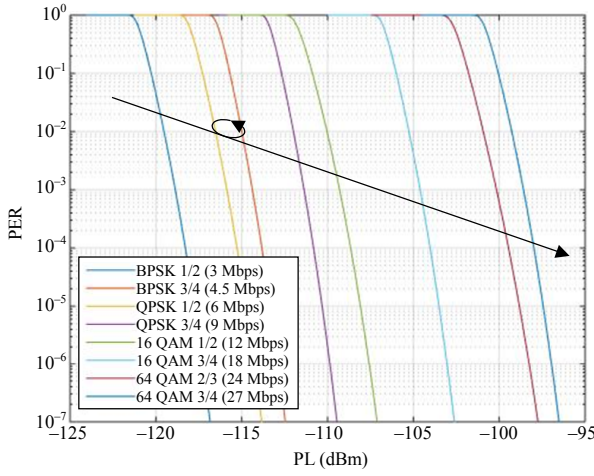


Fig. 9. PER vs. PL under an AWGN channel, where NF and $ImpLoss$ are 10 dB and 5 dB, respectively.

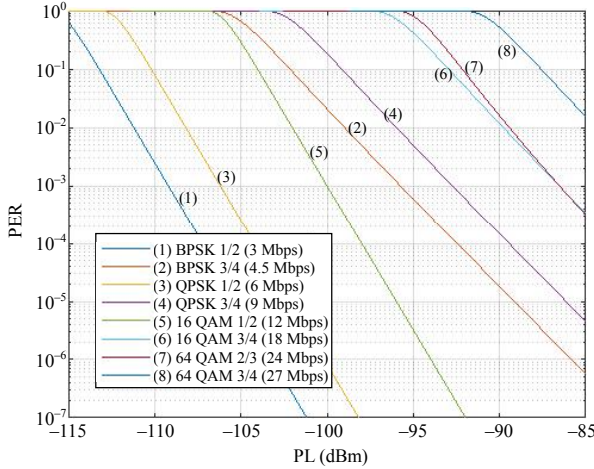


Fig. 10. PER vs. PL under a Rayleigh fading channel, where NF and $ImpLoss$ are 10 dB and 5 dB, respectively.

$$S_{RX} \left(\frac{E_b}{N_0} \right) - G_{RX} - E_{TX} = 10 \log_{10} \left| \frac{1}{2\beta d_L} e^{-j\beta d_L} + \frac{1}{2\beta d_R} \frac{\varepsilon_r \cos \theta - \sqrt{\varepsilon_r - \sin^2 \theta}}{\varepsilon_r \cos \theta + \sqrt{\varepsilon_r - \sin^2 \theta}} e^{-j\beta d_R} \right|^2. \quad (29)$$

The PER in terms of the V2V distance for an AWGN channel is shown in Fig. 11. The lowest PHY (MCS) mode (BPSK 1/2) can provide a link coverage of up to 1,500 km to meet a PER of 10%, whereas the highest PHY (MCS) mode (64 QAM 3/4) can reach approximately 450 m under the same conditions. It was observed that the link coverage rapidly decreases as the PHY (MCS) modes increase.

The PER in terms of the V2V distance for a Rayleigh fading channel is shown in Fig. 12. The increase in PER at around

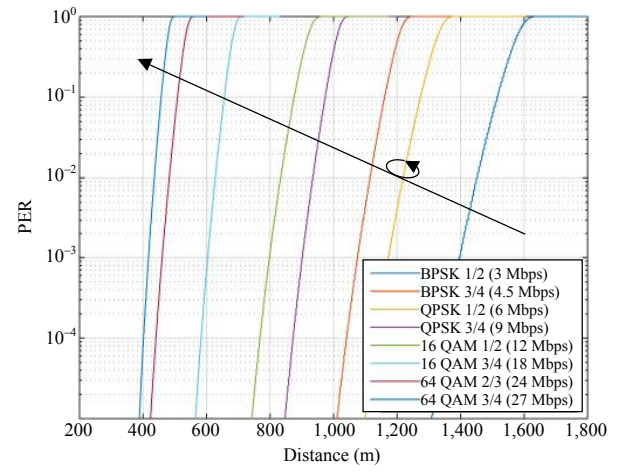


Fig. 11. PER vs. V2V distance for an AWGN channel using the 2-ray path loss model.

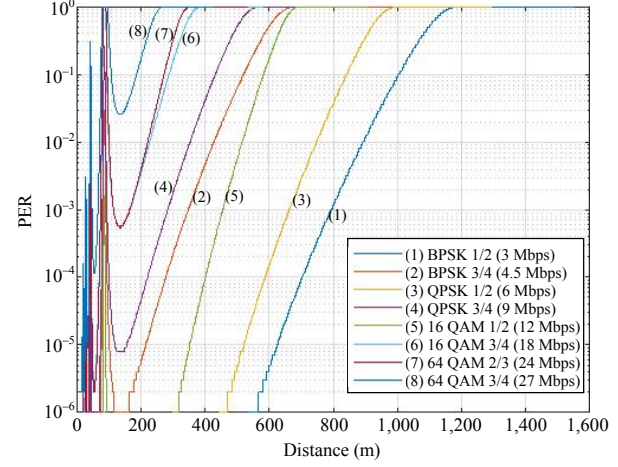


Fig. 12. PER vs. V2V distance for a Rayleigh fading channel using a two-ray path loss model.

100 m for the high PHY modes is caused by a sudden power drop in the two-ray path loss model.

IV. Maximum V2V Broadcast Throughput

It is instructive to determine the maximum V2V broadcast throughput in terms of distance when a path loss model is applied, which can provide guidance toward satisfying the QoS for a promising ITS service, such as a basic security message broadcast to different vehicles [26]. The analysis was conducted under the same assumptions as those described in Section II, with the exception that a transmitted packet error occurs because of the path loss in AWGN and fading channels. The maximum V2V broadcast throughput with the two-ray path loss model can be determined by following the steps listed in Table 6.

The throughput in terms of the V2V distance for an AWGN

Table 6. Steps used to calculate the maximum throughput using the PL model.

1. Preconditions to obtain DBs:
- Get DB for $PL(distance)$ from (25)
- Get DB for $PL(PER)$ for all PHY modes from (28)
- Get DB for MT_{ideal} from (4) for the broadcast case
2. Compute max. throughput for each PHY mode
for PHYmodes, m
for distance, d
Find $PL(d)$ for a given d
Find $PL(PER, m)$ to have the same $PL(d)$
Convert into $PER(PL, m, d)$ for given m and d
Find $MT_{PL}(m, d) = MT_{ideal}(m) \times [1 - PER(PL, m, d)]$
end
end

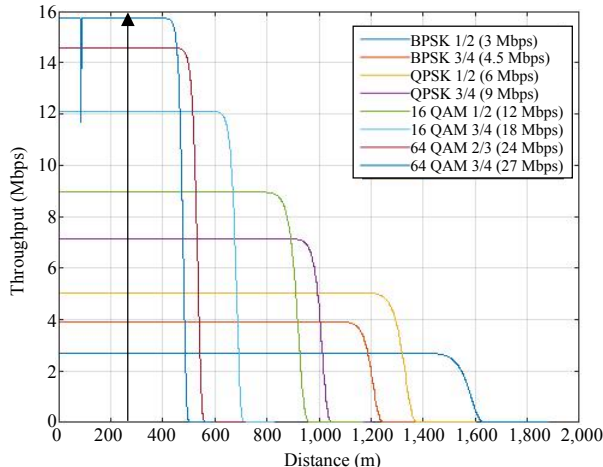


Fig. 13. Maximum throughput vs. the V2V distance for an AWGN channel using two-ray path loss model.

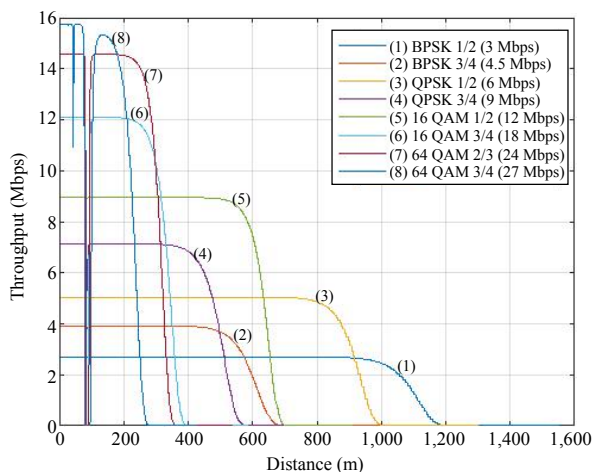


Fig. 14. Maximum throughput vs. V2V distance for a Rayleigh fading channel using two-ray path loss model.

channel is shown in Fig. 13. It can be seen that the higher PHY modes provide more throughput, while the coverage decreases. The capability of the PHY mode of 64 QAM 3/4 is 8 times greater than that of BPSK 1/2, although the coverage is only 1/3.

The throughput in terms of the V2V distance for the Rayleigh fading channel is shown in Fig. 14. The throughput coverage is much shorter than that for the AWGN channel. For the same PHY modulation, a coding rate of 3/4 obtains more throughput but less coverage compared to a coding rate of 1/2. The link coverage gap in the different coding rates for the same PHY modulation is larger than that for the AWGN channel.

V. Conclusion

In this paper, the performance of the WAVE system, which is a DSRC system based on the IEEE 802.11p standard, was discussed. The purpose of the analysis was to derive the maximum V2V broadcast throughput for AWGN and fading channels using a two-ray path loss model. A few assumptions were made to achieve the maximum V2V throughput, such as no packet collisions, the use of a full buffer model, and only packet drops caused by the degradation of the transmitted power in AWGN and fading channels. The upper bounds of the PER based on the WAVE system were derived using a Viterbi HDD to obtain more practical results. The analysis was performed using a two-ray path loss model and a simple topology, the maximum coverage of which was approximately 1,500 m and 1,100 m for AWGN and fading channels, respectively. It should be noted that other topologies can be evaluated by simply applying different path loss models. One interesting observation of note is that PHY modes with a high coding rate, such as 1/2, are more beneficial than those using 3/4 in terms of the throughput and coverage, particularly in fading channels. The performance results obtained, including the receiver sensitivity and link budget analysis, provide good insights into cell planning as well as the hardware performance requirements.

References

- [1] P. Papadimitratos et al., "Vehicular Communication Systems: Enabling Technologies, Applications, and Future Outlook on Intelligent Transportation," *IEEE Commun. Mag.*, vol. 47, no. 11, Nov. 2009, pp. 84–95.
- [2] IEEE802.11, *IEEE Standard for Information Technology—Telecommunication and Information Exchange Between Systems Local and Metropolitan Area Networks Specific Requirements Part11: Wireless LAN Medium Access Control (MAC) and Physical Layer (PHY) Specifications*, IEEE, Piscataway, NJ, USA, 2012.

- [3] Y.J. Li, *An Overview of the DSRC/WAVE Technology: Quality, Reliability, Security and Robustness in Heterogeneous Networks*, Huston, TX, USA: Springer Berlin Heidelberg, 2012, pp. 544–558.
- [4] J.B. Kenney, S. Barve, and V. Rai, “Comparing Communication Performance of DSRC OBEs from Multiple Supplies,” *ITS World Congress*, Vienna, Austria, Oct. 22–26, 2012, pp. 80–87.
- [5] ITS Joint Program Office, *Connected Vehicle Safety Pilot*, OST-R, US Department of Transportation, 2012, Accessed July 9, 2016. http://www.its.dot.gov/safety_pilot
- [6] Matthias Schulze, *Drive C2X*, European Commission, 2014, Accessed July 9, 2016. <http://www.drive-c2x.eu/project>
- [7] Y.S. Song, S.W. Lee, and H.S. Oh, “Performance Evaluation of WAVE Communication Systems under a High-speed Driving Condition in a Highway,” *J. Korea Inst. Intell. Trans. Syst.*, vol. 12, no. 3, 2013, pp. 96–102.
- [8] S.-C. Kim, “An Evaluation of the Performance of Wireless Network in Vehicle Communication Environment,” *J. Korean Inst. Commun. Inform. Sci.*, vol. 36, no. 10A, 2011, pp. 816–822.
- [9] J. Maurer, T. Fügen, and W. Wiesbeck, “Physical Layer Simulations of IEEE802.11a for Vehicle to Vehicle Communications,” *IEEE Veh. Technol. Conf.*, Dallas, TX, USA, Sept. 25–28, 2005, pp. 1849–1853.
- [10] Y. Zang et al., “An Error Model for Inter-vehicle Communications in Highway Scenarios at 5.9 GHz,” *ACM Int. Workshop Performance Evaluation Wireless Ad-hoc, Sensor, Ubiquitous Netw.*, Quebec, Canada, Oct. 10–13, 2005, pp. 49–56.
- [11] Y. Xiao and J. Rosdahl, “Throughput and Delay Limits of IEEE 802.11,” *IEEE Commun. Lett.*, vol. 6, no. 8, Aug. 2002, pp. 355–357.
- [12] E.S. Ha, “Throughput Analysis of Packet Applied to the Transmission Probability for CSMA/CA Protocol in Wireless LAN,” *J. Internet Comput. Services*, vol. 10, no. 1, 2009, pp. 51–61.
- [13] C. Campolo et al., “Modeling Broadcasting in IEEE 802.11 p/WAVE Vehicular Networks,” *IEEE Commun. Lett.*, vol. 15, no. 2, Dec. 2011, pp. 199–201.
- [14] Y.P. Fallah et al., “Analysis of Information Dissemination in Vehicular Ad-hoc Networks with Application to Cooperative Vehicle Safety Systems,” *IEEE Trans. Veh. Technol.*, vol. 60, no. 1, Oct. 2010, pp. 233–247.
- [15] X. Ma and X. Chen, “Delay and Broadcast Reception Rates of Highway Safety Applications in Vehicular Ad hoc Networks,” *Mobile Netw. Veh. Environments*, Anchorage, AK, USA, May 11, 2007, pp. 85–90.
- [16] Y. Wang et al., “Reliability Evaluation of IEEE 802.11 p-Based Vehicle-to-Vehicle Communication in an Urban Expressway,” *Tsinghua Sci. Technol.*, vol. 20, no. 4, Aug. 2015, pp. 417–428.
- [17] M.E. Renda et al., “IEEE 802.11 p VANets: Experimental Evaluation of Packet Inter-reception Time,” *Comput. Commun.*, vol. 75, Feb. 2016, pp. 26–38.
- [18] A. Goldsmith, “Wireless Communication,” Cambridge, USA: Cambridge University Press, 2005, p. 182.
- [19] S. Mangold, S. Choi, and N. Esseling, “An Error Model for Radio Transmission of Wireless LANs at 5GHz,” *Achen Signal Theory*, Aachen, Germany, Sept. 2001, pp. 209–214.
- [20] A.J. Viterbi, “Convolutional Codes and Their Performance in Communication Systems,” *IEEE Trans. Commun. Technol.*, vol. 19, no. 5, Oct. 1971, pp. 751–772.
- [21] J. Conan, “The Weight Spectra of Some Short Low-Rate Convolutional Codes,” *IEEE Trans. Commun.*, vol. 32, no. 9, Sept. 1984, pp. 1050–1053.
- [22] D. Haccoun and G. Begin, “High-Rate Punctured Convolutional Codes for Viterbi and Sequential Decoding,” *IEEE Trans. Commun.*, vol. 37, no. 11, Nov. 1989, pp. 1113–1125.
- [23] M.K. Simon and M.S. Alouini, *Digital Communication over Fading Channels*, Hoboken, NJ, USA: Wiley-IEEE Press, 2005, p. 24.
- [24] T.S. Rappaport, *Wireless Communications*, Upper Saddle River, NJ, USA: Prentice Hall PRT, 2002, pp. 120–125.
- [25] C. Dou and J.M. Chang, “An Analytical Model for Deriving Receiver Sensitivity and Minimum Transmit Power in 802.15.6 Wireless Body Area Networks,” *IEEE MTT-S Int. Microw. Workshop Series RF Wireless Technol. Biomed. Healthcare Applicat.*, Taipei, Sept. 21–23, 2015, pp. 138–140.
- [26] SAE J2945TM, *On-Board System Requirements for V2V Safety Communications*, SAE, Warrendale, PA, USA, 2016.



Yoo-Seung Song is a principal researcher at the Autonomous Vehicle Infrastructure Research Section in the ETRI, Daejeon, Rep. of Korea. He received the BS degree in electrical engineering from Changwon National University, Rep. of Korea, in 1996, and MS and PhD degrees in electrical and computer engineering from Wichita State University, KS, USA, in 1998 and 2001, respectively. From 2001 to 2005, he was with the Media Lab. of Samsung Electronics, Suwon, Rep. of Korea. Since joining ETRI in 2005, his work has been focused on next-generation WLAN, 3D-ray tracing, WAVE, C-ITS, and V2X Communications.



Hyun-Kyun Choi is a principal researcher of the Autonomous Vehicle Infrastructure Research Section, ETRI, Daejeon, Rep. of Korea. He received the BS and MS degrees in electronic engineering from Kyungpook National University, Daegu, Rep. of Korea, in 1995 and 1997, respectively, and the PhD degree in electronic engineering from Chungnam National, Daejeon, Rep. of Korea, in 2015. He joined ETRI in 2000. His research interests include intelligent vehicles, V2V, V2I communication, ITS, and PON.